J. Condensed Matter Nucl. Sci. 8 (2012) 105–114

Research Article

Quantum-correlated Fluctuations, Phonon-induced Bond Polarization, Enhanced Tunneling, and Low-energy Nuclear Reactions in Condensed Matter

K.P. Sinha

Physics Department (Emeritus), Indian Institute of Science, 560012 Bangalore, India

A. Meulenberg *

NAv6 Centre, Universiti Sains Malaysia, 11800 Penang, Malaysia

Abstract

In heavily (deuterated or hydrogenated) palladium, some of the crystallinity is lost. As a consequence, the localized phonon modes of the crystal/damaged-region interface have a much higher frequency than the host. These high-frequency modes create electrostatic fields that interact strongly with electrons of the local atoms. A resulting instantaneous potential inversion, from polarization, leads to the formation of lochons (local charged bosons–electron pairs in the singlet state, perhaps isolated from the Pd d-orbital energy levels) and of an associated H^+ or D^+ ion (with its two shared electrons instantaneously isolated into the adjacent Pd d-levels). The Coulomb repulsion between the nuclei of these pairs is greatly reduced by strong screening from the lochons that can even generate an attractive polarization potential. Furthermore, the mutual tunneling penetration probability of the Coulomb barrier is enhanced by correlated fluctuations. This arises from the generalized uncertainty relations, $\Delta x\ \Delta p_x$, $\Delta E\ \Delta t \geq (n + 1/2)h/(1 - \rho^2)^{0.5}$, where n may be on the order of 10–100 and where results from two models are combined. The integer n values represent excitations in the phonon modes of the H or D sub-lattice and ρ is the correlation coefficient with $0 < \rho < 1$. Higher values of $n$and ρ, for a particle in a potential well, imply less localization and greater uncertainties in location (i.e., extending its probability distribution further into the barrier). These periodic fluctuations into the barrier are an interference effect similar to that of beat frequencies.
 ISSN 2227-3123

Keywords: Bond polarization, Correlated fluctuations, Lattice-assisted tunneling, LENR, Phonons

1. Introduction

As noted earlier, low-energy nuclear reaction (LENR) occurs in PdD_x (or PdH_x) after considerable loading by D or H [1]. This loading produces degradation of crystallinity or amorphization of the alloy [2]. When extreme, this degradation is known to suppress LENR by allowing H_2 or D_2 to escape from the interior of the crystal along fractures. On the

*E-mail: mules333@gmail.com; Tel.: 011-604-6534632

 ISSN 2227-3123

other hand, disorder at a lower level may provide some of the necessary conditions for LENR. With this in mind, one has to consider not just the bulk material, but, also its external surfaces, its defects, and its internal crystallite and grain boundaries [3]. Of particular interest at these boundaries are the defects and the interface phonon modes. Associated with the boundary, interface, and defect states is the effect of nanoparticle (NP) surfaces relative to those of bulk or even thin-film material. The large surface to volume ratio of the NPs, relative to Pd thin films and bulk, alters the Pd-lattice size and its response to hydrogen loading [2]. At least in this recent study, the PdH_x beta phase in NPs appears to be dominant at exposure to 2% H gas, but not until 10% H gas for thin films. Thus, both surface and subsurface effects depend on the nature of the interfaces. Linear defects have been addressed earlier [4]. The present paper examines another aspect of these interfaces.

2. Generalized Uncertainty Relation

The wave amplitude of interface phonon modes (in particular, longitudinal-optical modes) decays away from the interface junction. Thus, solutions of the wave equation correspond to localized modes near the interface. Further, these phonons produce electrostatic fields that strongly couple with the electrons and ions confined to the layer in a manner that may differ from that in the bulk. The effect of these fields in introducing paired-electron states (lochons – local charged bosons) has been discussed in detail in earlier papers [5,6]. Here we also explore the local-interface-state phonons as distinct from the bulk phonons.

The frequencies (ω_1) of these localized modes are much higher than those of the phonon modes of the pure (host) lattice [7].In addition to the higher frequency (energy) of the local-state phonons, we will explore the effects of the phonon populations and of their correlations. Since we are concerned only with these localized-longitudinal-lattice modes, we will just use $\omega_1 = \omega$ in the equations below.

The expectation values of the number of these phonons at a particular frequency $\langle n_{r,\omega}\rangle$ about an interface D* or H* sub-lattice atom (or ion) and the expectation values of their amplitudes $\langle A_{r,\omega}\rangle$ are related [7].

$$\langle n_{r,\omega}\rangle = 2M\omega\langle A_{r,\omega}\rangle^2/\hbar, \tag{1}$$

where M is the mass of the atom. For $M_{\mathrm{D}} =\sim 3.3 \times 10^{-24}$ g, $\omega \simeq 5 \times 10^{14}$ to 10^{15} s^{-1} and $\langle A_{r,\omega}\rangle =\sim 3 \times 10^{-9}$ cm, $\langle n_{r,\omega}\rangle$ is of the order of tens of phonons. Why do we choose this value for A? If the spacing between the interstitial D site and the lattice barrier containing the deuterium is on the order of 10^{-8} cm, then a quadratic potential well, with a broad minimum would allow motion within its walls that would be dependent on the square root of the energy, e.g., on the number of phonons in a given direction and frequency (defining a mode). With many variables determining the actual average motions (temperature, direction, etc.), a ball-park value is the best that can be suggested. While the room-temperature mean-squared displacement [8] is ~ 0.09 au $= \sim 5 \times 10^{-10}$ cm, the transitory displacement into preferred directions (e.g., between Pd atoms and with another polarized deuterium atom approaching from the adjacent cell) will be significantly greater. The lattice-assisted nuclear reaction, LANR, depends on this increased displacement and the 'additional effects' mentioned below.

In the context of the present problem, we have to consider the time (t) energy (E) uncertainty relation as generalized by Schrodinger [9] and Robertson [10] and extended by Roy and Singh and others [11–13]. Since the maximum energy in phonons of a given mode is equal to the sum of the n phonons plus the zero-point energy ($\hbar\omega/2$) of the mode (ω), and each phonon has $E = \hbar\omega$, and the cycle time is inversely proportional to (ω), then:

$$\Delta x\ \Delta p_x \text{ and } \Delta E\ \Delta t \geq (n_{r,\omega} + 1/2)h. \tag{2}$$

Accordingly, the fluctuation-enhanced uncertainty in energy (the dynamic portion of the phonon that goes through zero twice a cycle) turns out to be:

$$\Delta E > (n_{r,\omega} + 1/2)h/\Delta t =\sim 2M_{\mathrm{D}}\omega\langle A_{r,\omega}\rangle^2/\Delta t. \tag{3}$$

It now becomes important to determine the appropriate value of Δt. Since E varies between 0 and $E_{\max}$ in 1/4 of a cycle, the time of that maximum uncertainty should also be 1/4 of a cycle. With $\omega = 2\pi\upsilon > 0.5 - 1 \times 10^{15}$ rad/s, we can assume a period of $T = \sim 10^{-14}$ s and $\Delta t = \sim 2 \times 10^{-15}$ s. With values of the other parameters given above, we have $\Delta E = 1.5 - 3 \times 10^{-11}$ ergs = $\sim 10 - 20$ eV. This energy is very high for phonons and even for plasmons. However, when we take into account the polarization-induced dynamic, short-range, attractive forces (Eq. (A.4) in the Appendix) of the deuterium and the Pd atoms near the collision point of the lattice barrier, the value is more realistic. Furthermore, this is close to the $\sim$ 40 eV associated with the plasma frequency of the Pd electron cloud [14].

If the preferred directions are along a linear harmonic chain (spacing = a), then with only nearest-neighbor interaction, oscillations $\omega(k) = \omega_0 |\sin(ka/2)|$ result, where ω_o is the resonance frequency. The phonon density of this level (density of normal modes) [15] is given by $g(\omega) = 2/\pi a(\omega_0^2 - \omega^2)^{1/2}$.ghe number of phonons in this 'van Hove singularity' is limited by many things; but, populations in resonant states can still be high. By increasing the local fields and displacement amplitudes, such resonance may greatly enhance the polarization potential $V_{\rm pp}(r)$ [16].

Tunneling probabilities in the classically forbidden region will have the form

$$P(E) = \exp[(-2/\hbar)\int (2M(V(r) - E))^{1/2} \mathrm{d}r_i]. \tag{4}$$

Taking the above polarization and fluctuation into account, the factor $(V(r) - E)$ changes to

$$V(r) + V_{\rm pp}(r) - \Delta E(\rho) - E, \tag{5}$$

where $V_{\rm pp}(r) = -|\alpha|^2/2r^4$ is an attractive short-range potential (Appendix).Even for low-energy situations, where E is almost negligible compared to $V(r)$, the phonon-induced $\Delta E(\rho)$ can rise to the tens-of-eV range. The difference between this and the $\sim$ 26 meV of room temperature energy, generally considered in such problems, may increase the tunneling probability of D–D fusion by many tens of orders of magnitude.

It is interesting that this result, when combined with the low energy, zero angular momentum corrections [4] to the normal Gamow tunneling-cross-section equation, corresponds roughly to those results predicted by the high values of ΔE ($\sim$ 400 eV) determined by low-energy deuteron-beam experiments and the uncorrected Gamow equation [17]. The researchers involved in such experiments attribute the result to screening of the D–D interactions by electrons of the embedding material. *However, theoretical calculations for conventional screening effects are only one-quarter to one-half of these experimental values*. Screening effects, addressed in the next section, are not included in these calculations above.

3. Correlated Fluctuation

Phonons, as bosons, are self-correlating when in the same mode. That is why their ability to transfer energy is additive. However, any lattice has many modes. Not being in the same state as in other modes, most phonons do not necessarily add. However, if they are correlated, they can phase lock because of the non-linearities within a lattice and become coherent. A subset of these correlated phonons, the longitudinal-optical mode, is of particular interest to us.

An example of the consequences of this coherence is pictured by considering the probabilities of deuterons penetrating the lattice barrier if their periodic motion is in phase with a periodic motion of the Pd atoms. If the phases are such that the Pd atoms are further apart [18] at the time that the D atoms are approaching the barrier, the penetration will be much greater than if either phase were reversed. If these particular phonon frequencies of the Pd and D lattices are equal, or harmonic, then the number of deep penetrations for in-phase motion is increased relative to that of non-resonant phasing.

To carry this picture into the real world, assume the motion modes are not independent. This is likely, since real potentials are not truly simple harmonic oscillators (as generally assumed in QM). The anharmonicity or non-linearity of

the modes may allow them to couple to other modes (or result from such coupling). Even anharmonic correlation of the modes will create periodic fluctuations large enough to permit fusion under the right circumstances. Such events would just happen less often than they would with harmonic correlations. If the modes are of equal or multiple frequencies, the coupling can grow and reach a folding point (something breaks). Does this apply to the LANR experiments? Two examples described below indicate that this may be so.

Experiments with laser stimulation of deuterium sub-lattice phonon modes (using beat frequencies of laser pairs to get into the correct frequency range [19]) have demonstrated enhanced heat output at specific ranges. This is expected from any model based on lattice barrier penetration by deuterons. However, stimulation of PdD by lower frequencies, e.g., those produced by complex acoustic stimulation [20] (deliberately constituted to create high-frequency overtones) and even high-frequency electrical stimulation [21] have also shown positive results.

These lower frequencies could stimulate the Pd-lattice resonant modes and thereby enhance the motion that could permit the deuterons greater access to adjacent sub-lattice sites. They could also stimulate the much higher deuteron phonon harmonic frequencies that are many multiples of the Pd-phonon and source frequencies. However, the sub-lattice frequencies that are most critical may be harmonics generated by non-linearities of the Pd phonon modes and would then have both the correct frequencies and phase relationship for enhanced deuteron transport into and across the lattice barriers.

What are the quantitative consequences of this coherent-correlation effect? Given a correlation factor ρ, where $0 \leq \rho < 1$, that increases with correlation, we find an effect on the uncertainty relation such that

$$\Delta E\, \Delta t = \Delta x\, \Delta p_x \geq \hbar/2(1-\rho^2)^{0.5}. \tag{6}$$

This means that as correlation increases, the fluctuations in energy, time, position, or momentum increase as well. For highly correlated states in which $\rho \Rightarrow 1$, the fluctuations in position or momentum can be quite high. If the states are also coherent, then these fluctuations can seldom occur or can occur all of the time (every cycle or n^{th} cycle) depending on the phase and harmonic. If we couple the phonon effects with the correlated-coherence effects, then Eq. (2) becomes:

$$\Delta E\, \Delta t = \Delta x\, \Delta p_x \geq (n_{r,\omega} + 1/2)\hbar/(1-\rho^2)^{0.5}. \tag{7}$$

If n is of order 10 and ρ is 0.9, the fluctuations in energy, relative to standard calculations, can increase by $\sim 20\times$. This value can be larger and readily enhanced. Specifically, the effects of proper laser stimulation of phonon modes can greatly increase $n_{r,\omega}$ and the selection, modifications, and chance correlation of material properties can be explained and shown to contribute greatly to the energy of the deuteron fluctuations within a Pd lattice.

4. Additional Effects

There are combined effects that might go beyond the non-linearities that can couple orthogonal modes. For example, if the optical modes of the Pd lattice allow the lattice barrier to be lowered at a time when the deuteron pair is approaching it, the amplitude of oscillation in that particular deuteron lattice mode may be significantly increased. The increased amplitude does not necessarily mean that the number of phonons increases in this case (Eq. (8)). The effective mass of the deuterons could be altered by the motion of the Pd lattice. Barrier penetration attributed to stochastic extremes [22] could, in fact, be a result of these coherent-correlated effects. There are so many variables in this problem that it is unlikely that theory alone will be able to determine which is most important (until experimental results point the way).

Beside the mechanical resonances that are obviously important, there are electric field effects of the phonons that may be even more important for the heat versus fragmentation balance in any resulting D–D fusion. Palladium, as a metal, clearly has many or most of its lattice atoms ionized. Hydrogen, with its much deeper ground-state energy levels, would not be ionized much, if any, of the time. However, it shares its electron with the adjacent ionized-Pd atoms. The Pd ion(s) also shares d-orbital electrons with the H atom. This results in a covalent bond sharing the H ground-state

orbital and yet leaving it with a net positive charge in the lattice [23,4]. The polarized covalent bond between the H and Pd atoms raises the average H energy level (Appendix) and population of the Pd valence electrons and therefore increases the conductivity of the material as H is added (nearly up to saturation, at $x = 1$ in PdD_x). Pd-ion and PdD-dipole phonon modes will generate oscillating electric fields. These fields interact with the H or D electrons, thereby polarizing the deuteron pairs colliding (at a Pd lattice barrier) in the longitudinal optical-phonon modes. The phonon-induced colliding motion of the H (or D) atomic pairs in the sub-lattice, means that the bound electrons, attracted to the opposing D nucleus will do more work (W = Force $\times$ distance, T. Barnard, http://www.ichaphysics.com/the-science-of-cold-fusion] than they could without the phonon assist.[a]

An aspect of this $\boldsymbol{E}$-field interaction that ties in with the correlated-coherent phonon modes and the deep orbit is the Extended Lochon Model [24]. This model makes use of these fields to create stable hydrogen–electron pairs in an s-orbital that is momentarily, but cyclically, much below the Pd d-orbitals. This periodically decouples the D–Pd covalent bonds and creates a D^- ion within the lattice. Similarly, the fields can momentarily polarize valence electrons away from an adjacent lattice and sub-lattice location. This means that the shared Pd and D electrons shift more toward the Pd atoms leaving these D atoms/ions with a greater net positive charge. The result is a D^+D^- pair that is attractive and aids in the collision process by reducing the Coulomb barrier in size and magnitude. Thus, coupled-phonon modes, which might not appear to have any mechanical connection with the deuterons' motion toward the lattice barrier, may have a major role simply by altering the electron concentration/polarization in the right place at the right time.

The above examples provide physical intuition for the theoretical papers on coherent-correlated-enhancement[12] and anharmonic-fluctuation effects. These dynamic resonance and non-linear effects are seldom treated well in QM because they are so dependent on material properties. Therefore, it is an open question as to which is more likely to succeed in determining the best materials and conditions for LENR and LANR, theory or experiment. Here-to-fore, experiment has provided the only basis for moving forward. Only now, is there a glimmer that theory can help guide in the selections.

5. Strong-screening Contribution

In our earlier papers [3–6], we have invoked the concept of strong-screening and attraction as a result of the doubly negative lochon being present in a tight orbit about a deuteron. The advantage of this concept is that the electron effective size and orbits shrink as the colliding deuterons approach on another. They shrink for two reasons. First, the long-range Coulomb fields of the electrons and protons cancel each other more completely as they approach one another. The screened long-range monopole charge field becomes a short-range dipole field. Second, if the electrons do work on bringing the deuterons together, they move deeper into the potential well converting potential energy into kinetic energy and work. This lowers the orbit radius. At the sub-atomic level, shrinking the average electron distance from the nuclei, which determines the 'effective size' of the electron, has the greatest effect on tunneling probability by reducing the length of the nuclear-Coulomb barrier..

There is a point to our considering that electrons reduce their average distance from a nucleus just by doing work. It allows them to reach the postulated deep-electron location (at least a metastable or resonance state), which is not accessible by normal means, i.e., photon emission [25]. It is also expedient to consider that a strong-screening effect of these tightly bound electron pairs is created assuming a lochon in this deep orbit.

The local screening effect may be represented by an equation normally used to describe an 'effective charge' of a unit charge in a plasma or free electron environment:

$$e^2 \rightarrow (e_{\text{eff}})^2 = e^2 \exp(-\alpha_s), \tag{8}$$

[a]Without phonon assist, the electrons move in the atomic Coulomb potential, not the nuclei; thus, the work they do is generally negligible. If the phonons move the nuclei, then the work done by the electrons can be significant.

where α_s is the dimensionless screening parameter [26]. This α_s is not the same as the polarizability α in the appendix; however, it is very similar in both nature and effect. Values of $\alpha_s = 1, 2$, which give $e_{\text{eff}} =\sim e/2$, provide screening sufficient to raise the energy level of a bound hydrogen electron pair beyond their binding energy. In the presence of the electron pair's bound double-negative charge, what is the effective charge of the deuterium nucleus as seen by another charge. Since H^- in the lattice is instantaneously stable, the paired electrons must be in a much deeper orbit or at least not provide the same value of e_{eff} as would a free-electron density giving $\alpha_s = 1.2$. However, since the lochon model requires close proximity of the second deuteron to bring the lochon to a deep orbit, the paired deuterons must already be very close together. For even instantaneous stability at this point, the new screening parameter, α'_s, is once again on the order of 1 and the effective charge of one of the deuterons (as seen by the other) is $e_{\text{eff}} =\sim 0.6e$.

For the H^- and D^- lochon cases, our estimated value of $\alpha'_s (\sim 1)$, gives $e^2 \exp(-\alpha_s) = 23 \times 10^{-20} \times 0.37 =\sim 8 \times 10^{-20}$ esu. Thus, to reach a micro-molecule orbit (e.g., $\sim 2 \times 10^{-11}$ cm) at which point fusion occurs rapidly, the nuclei have to climb a Coulomb barrier of energy:

$$V(R) = e^2 \exp(-\alpha_s)/R =\sim 8 \times 10^{-20}\,\text{esu}/2 \times 10^{-11}\,\text{cm} = 4 \times 10^{-9}\,\text{erg} = \sim 3\ \text{keV}. \tag{9}$$

This is compared to the ~ 10 keV at which D–D colliding beam experiments start seeing measurable deviations from the Gamow tunneling model. The actual attraction and repulsion of the electron charges with the protons and each other must be examined in this context, since the protons will screen the electrons as well.

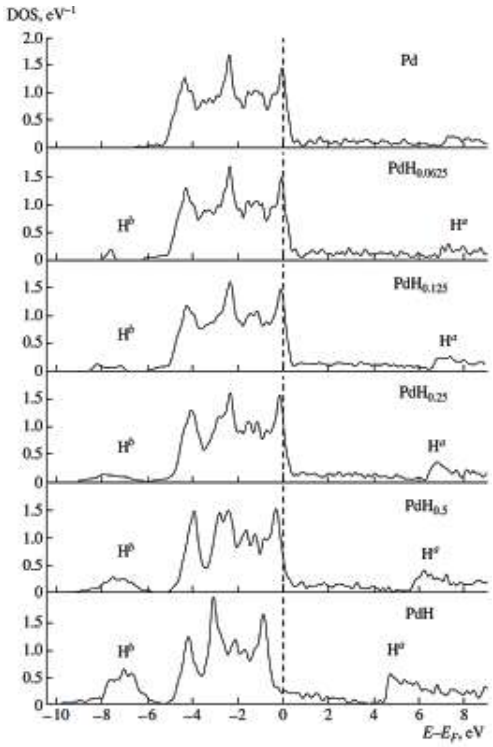

Figure 1. Density-of-states, DOS, in pure Pd and in PdH_x solid solutions for different H concentrations x. H^b and H^a are peaks corresponding to bonding and antibonding states of Pd–H ([28] with permission).

.

6. Conclusions

It is seen that no single mechanism can account for the D–D fusion observed in cold-fusion experiments. However, a combination of effects can explain some of the results. Individual phonons are below the 100 meV range; however, as bosons, they seek the same states and can increase the effective energy of their combined action by more than an order of magnitude. Random fluctuations of the lattice-barrier height can permit deuterons to penetrate the barrier, if they are at the right place at the right time. This is unlikely for truly random fluctuations. Therefore, it is important to seek correlated and coherent motions of the deuterons and Pd atoms within the lattice.

If the motions (phonon-induced) are both coherent and correlated, then resonance effects can greatly amplify the deuteron motions within the sub-lattice. If Pd lattice phonons are also coherent and correlated (at least harmonically) with the sub-lattice phonons, then the lattice barriers can be greatly lowered at the correct times for barrier penetration by the deuterons.

Even if the motions of the deuterons and the Pd lattice are correct for barrier penetration, the deuterons cannot overcome their nuclear Coulomb barrier without other mechanisms. The phonon electric fields can provide one of these by cyclically polarizing the deuteron electrons relative to the colliding deuterons. As a result, if the different phonon modes of both the lattice and sub-lattice allow coherent-correlated action, the bound electrons can move deeper into the nuclear-Coulomb-potential well for hundreds of orbits and shrink their orbital radius during a portion of the phonon cycle. This action leads to a strong-screening effect, or actual attraction between the deuterons, that reduces the effective charge of the nuclei and allows them to penetrate through their mutual Coulomb barrier to the attractive nuclear potential well within.

The LENR results, both from the unconventional 'Cold Fusion' community and the 'conventional' keV D–D collision work, cannot be explained by standard mechanisms. The cumulative effects on the energy barrier proposed in this paper are still small compared to those effects from standard calculations, 10s of eV vs ∼100 eV for screening, that can enhance fusion results. And these, in turn, are small compared to the experimental values attributed to screening to explain fusion rates for low-energy (> keV) D–D collision experiments [17]. Therefore, there must be a difference between the random nature of screening and the actual cause of the high fusion rates observed. Reducing the randomness and 'focusing' the effects of the low energies available in the system appear to be key to the observed LENR results. Even these contributing factors are not likely to be sufficient unless some other mechanism is, or can be, triggered by the additional energies and mechanisms. The ability of the electron pairing (formation of the lochon), to not just overcome

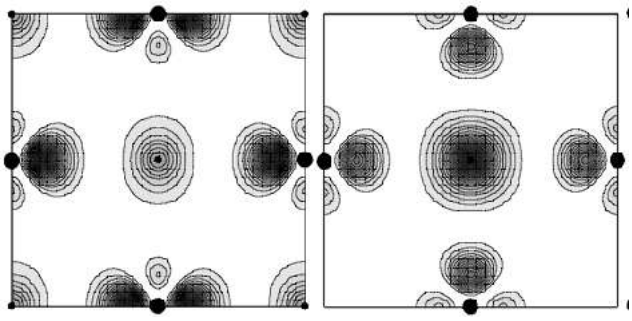

Figure 2. Maps of electron probability-density distributions for H-–Pd bonding and anti-bonding states in PdH (*left panel*) and PdH 0.25 (*right panel*). The four large dots in each frame represent Pd atoms and the 5, or 1, small dots represent H atoms. ([28] with permission)

the Coulomb barrier problem but to create an attraction between deuterons under the proper conditions, would appear to be the mechanism that can explain the observed fusion rates. This mechanism also leads to answers [24] of the arguments against LENR based on known high-energy nuclear physics.

Acknowledgement

This work is supported in part by HiPi Consulting, New Market, MD, USA; by the Science for Humanity Trust, Bangalore, India; the Science for Humanity Trust Inc., Tucker, GA; a research grant from the Universiti Sains Malaysia – #1001_PNAV_817058 (RU); and the Indian National Science Academy.

Appendix A. Polarization and Electron-sharing Effects

In the situation of Pd loading by D (or H), one must take into account the polarizability of atoms, covalently bonded molecules, and clusters of atoms. Polarization leads to an attractive (induced-dipole) [27] potential:

$$V_{\mathrm{pp}}(r) = -\alpha e^2/2r^4, \tag{A.1}$$

where α is the polarizability having the dimension of volume. This will act: against the linear, hard-core, repulsive potential $V(r) = e^2/r$, between the nuclei of two interacting atoms (ions); and against the lattice barrier(s).

The tunneling probability in the classically forbidden region has the form

$$P(E) = \exp\left[-2/\hbar)\int_r^R \sqrt{2M(V(r)-E)}\,\mathrm{d}r\right], \tag{A.2}$$

where $E$is the energy of the deuteron and r_o and R denote the beginning and the end of nuclear-Coulomb potential barrier. For low-energy situations, E is almost negligible. However, when we consider the lattice, the situation is much more complicated. E now includes the minimum lattice barriers $V_l(r)$ and maximum energies. The average lattice energy may be at room temperature; but, with correlated motion and fluctuations (phonons and plasmons, etc.) arising from the generalized uncertainty, instantaneous energies $\Delta E(\rho)$ can be many eV. These energies can reduce the Coulomb barrier of the nuclei and lattice (assumed to be quadratic) and contribute to bringing adjacent deuterium atoms in the lattice closer together. Localized charge distributions increase the polarization potential $V_{pp}(r)$; and the factor $(2M(V(r) - E)^{0.5}$ for free-space is now modified to:

$$2M(V(r)-E)^{0.5} \Rightarrow (2M(V_1(r) + V_{\mathrm{pp}}(r) - \Delta E(\rho)))^{0.5}. \tag{A.3}$$

The values of $V(r)$, $V_l(r)$, and $V_{pp}\,(r)$ are compared (Table 1) for r values (distance between the H atoms approaching a common point of the lattice barrier) from $\sim 1.4 \times 10^{-8}$ to 7×10^{-9} cm. However, even with detailed modeling [8], predictions of potentials at $< 1.6 \times 10^{-8}$ cm are not considered to be reliable. Assuming unit charges and a value of deuterium polarizability to be $\alpha = 0.68 \times (10^{-8})^3$ – not generally valid in the solid state – an approximation gives Table 1.

Table 1. Comparison of potentials in Eq. (A.3)

	$V(r)$ (eV)	$V_1(r)$ (eV)	$V_{\mathrm{pp}}(r)$ (eV)
$r = 1.4 \times 10^{-8} \Rightarrow$	~ 7	~ 4	-1.2
$r = 10^{-8}$	~ 14	~ 4	-5
$r = 7 \times 10^{-9}$	~ 28	~ 4	-20

All of the potentials $V(r)$, $V_l(r)$, and V_{pp} (r) and ΔE are cyclic, but generally at different frequencies. In this region, they are similar in amplitude as demonstrated by the ability of hydrogen to diffuse in a Pd lattice and for plasmon-induced ionization to move throughout the lattice [29].

The attractive polarization potential gives rise to forces with which the interacting atoms (ions) move towards each other.

$$F_{\mathrm{pp}} = 2\alpha e^2/r^3. \tag{A.4}$$

With heavy loading, there is breakdown of crystallinity resulting from the amorphization of the alloy along with cluster formation. This can further increase the polarization and decrease the minimum distance of approach between deuterons.

Loading the Pd lattice with hydrogen, introduces an electron s-band below the Pd d-band (Fig. 1) [28]. Hybridization of these levels satisfies the atoms by 'filling' both the H s-orbitals and the Pd d-orbitals. However, the electrons are more tightly bound to the H atoms, and the result is a net negative charge on the H atoms relative to the Pd atoms. But, because of the loss of electrons to the conduction band, there is positive charge on both the Pd and H atoms. This relative charge difference produces a polarizable charge dipole that responds to both plasmon and photon fields. Because of the additional covalently-bonded electron in the hydrogen orbits, its induced polarizability is also greater.

As the H content increases with loading and the Pd d-orbitals fill, the Fermi level rises. Conduction eventually (at PdH) takes place only in the Pd 5s-orbital. While H does not 'lose' electrons in PdH, it shares electrons in a covalent bond with Pd atoms in a manner that makes it more positive than neutral atoms. Figure 2 displays the electron configurations about the Pd atoms (large dots) and H atoms (small dots) for PdH and for $PdH_{0.25}$. The electron density about the H atoms in $PdH_{0.25}$ (no H in corners) is greater than that in the PdH because, in the PdH lattice, there are fewer Pd electrons for each H to share.

Another explanation for the change in electron density about the hydrogen atoms is based on lattice strain. Until the Pd lattice is stressed by being filled, the hydrogen 1s- and the Pd 4d-orbitals do not spread sufficiently for them to overlap and share their electrons. Thus, the electrons are more confined than they are when the lattice is full.

A phonon-induced electric field can shift the shared electron(s) from one Pd or H atom (or pair of atoms) to another. Thus, H can change from bonding, H^b, to anti-bonding, H^a, states (Fig. 2). Since the charge densities differ about the H^b and adjacent H^a atoms, they will become polarizable as pairs and respond to the local fields. The H^a sites are dominant plasmon centers [29] and, if resonant with longitudinal optical-phonon modes, can have correlated-coherent effects that would greatly enhance the H–H or D–D fusion probability.

References

[1] M.C.H. McKubre and F.L. Tanzella, Cold Fusion, LENR, CMNS, FPE, One perspective on the state of the science based on measurements made at SRI, *J. Condensed Matter Nucl. Sci.* **4** (2011) 32–44.

[2] Manika Khanuja et al., Hydrogen induced lattice expansion and crystallinity degradation in palladium nanoparticles: Effect of hydrogen concentration, pressure, and temperature, *J. Appl. Phys*. **106** (2009) 093515-1to 8.

[3] K.P. Sinha and A. Meulenberg, Laser stimulation of low-energy nuclear reactions in deuterated palladium, *Current Sci.* **91**(7) (2006) 907–912 (arXiv:cond-mat/0603213).

[4] K.P. Sinha and A. Meulenberg. A model for enhanced fusion reaction in a solid matrix of metal deuterides, in *Proc. ICCF-14 Int. Conf. on Condensed Matter Nucl. Sci.* Aug. 2008, Washington, DC, D.J. Nagel, M. E. Melich, R. W. Johnson, S. R. Chubb, and J. Rothwell (Eds.), http://www.iscmns.org/iccf14/ProcICCF14b.pdf. ISBN: 978-0-578-06694-3.

[5] K.P. Sinha, *Infinite Energy* **29** (2000) 54 (arXiv:0705.0595v1).

[6] K.P. Sinha and A. Meulenberg, Lochon catalyzed D–D fusion in deuterated palladium in the solid state, *Nat. Acad. Sci. (India) Lett.* **30**(7,8) (2007) 243–245 (arXiv:0705.0595v1).

[7] L. Mihaly and M.C. Martin, *Solid State Physics*, Wiley-VCH, Weinhein, 2004.

[8] A. Shabaev, D.A. Papaconstantopoulos, M.J. Mehl and N. Bernstein, First-principles calculations and tight-binding molecular dynamics simulations of the palladium–hydrogen system, *Phy. Rev.* B **81** (2010) 184103.

[9] E. Schrodinger, *Ber. Kgl. Akad. Wiss, Ion*. (Berlin) **24** (1930) 296.
[10] H.P. Robertson, A general formulation of the uncertainty principle and its classical interpretation, *Phy. Rev.* **35** (1930) 667; An indeterminacy relation for several observables and its classical interpretat, *Phy. Rev.* **46** (1934)794–800.
[11] V.V. Dodonov, E.V. Kurmystev and V.I. Manko, Generalized uncertainty relation and correlated coherent states, *Phy. Lett.* A **79** (1980) 150.
[12] V.I. Vysotskii and S.V. Adamenko, Correlated States of Interacting Particles and Problems of the Coulomb Barrier Transparency at Low Energies in Nonstationary Systems, *Tech. Phys.* **55** (2) (2010) 613–621, ISSN 1063_7842, © Pleiades Publishing, Ltd., 2010; V.I. Vysotskii and S.V. Adamenko, *Zhurnal Tch. Fiz.* **80** (2010) 23.
[13] S.M. Roy and V. Singh, Generalized coherent states and the uncertainty principle, *Phy. Rev.* D **25** (12) (1982) 3413.
[14] S. Feng, Enhancement of cold fusion rate by electron polarization in palladium deuterium solid, *Solid State Communi.* **72**(2) (1989) 205–209.
[15] N.W. Ashcroft and N.D. Mermin, *Solid State Physics*, Holt, Rinehart and Winston, New York, 1976.
[16] K.D. Bonin and V.V. Kresin, *Electric-Dipole Polarizabilities of Atoms, Molecules, and Clusters,* World Scientific, Singapore, 1997.
[17] K. Czerski, A. Huke, P. Heide and G. Ruprecht, Experimental and theoretical screening energies for the ^{2}H(d, p)^{3}H reaction in metallic environments, *Eur. Phys. J.* A **27** (2006) s1.83–s1.88.
[18] E. Simanek, Quantum tunneling through a fluctuating barrier: enhancement of cold-fusion rate, *Physica* A **164** (1990) 147–168.
[19] D. Letts, D. Cravens and P.L. Hagelstein, Dual Laser Stimulation and Optical Phonons in Palladium Deuteride, *Low-Energy Nuclear Reactions and New Energy Technologies Sourcebook:* Vol.2, Marwan, Jan and Krivit, Steven B. (Eds.), American Chemical Society/Oxford University Press, Wash., D.C., 2009, pp. 81–93, DOI: 10.1021/bk-2009-1029.
[20] I. Dardik et. al., Ultrasonically-excited electrolysis experiments at energetics technologies, in *Proc. ICCF-14 Int. Conf. on Condensed Matter Nucl. Sci.*. Aug. 2008, Washington, DC, D.J. Nagel, M.E. Melich, R.W. Johnson, S.R. Chubb and J. Rothwell, http://www.iscmns.org/iccf14/ProcICCF14b.pdf, ISBN: 978-0-578-06694-3,
[21] R.E. Godes, Quantum fusion hypothesis, in *Proc. ICCF-14 Int. Conf. on Condensed Matter Nucl. Sci.,* Aug. 2008, Washington, DC, D.J. Nagel, M.E. Melich, R.W. Johnson, S.R. Chubb and J. Rothwell (Eds.),
http://www.iscmns.org/iccf14/ProcICCF14b.pdf, ISBN: 978-0-578-06694-3
[22] S. Habib, Quantum diffusion, *Proc. 4th Drexel Symposium on Quantum Nonintegrability*, 1994 (arXiv:hep-th/9410181).
[23] W. Sanger and J. Voitlander, Comparison between the magnetic susceptibilities of Pd_{1-x}, Ag, and single phase PdH, The 3:2 split of added electron ⇒ unbalanced covalent bond (s–d) *J. Magnetism Magnetic Materials* **71** (1987) 111–118.
[24] A. Meulenberg and K.P. Sinha, Tunneling beneath the ^{4}He* fragmentation energy, *J. Cond. Matter Nucl. Sci.* **4** (2011) 241–255.
[25] A. Meulenberg and K.P. Sinha, From the naught orbit to He* excited state, this issue, *J. Cond. Matter Nucl. Sci.* **5** (2012).
[26] S. Ichimaru, *Statistical Plasma Physics, Vol. II, Condensed Plasma*, Chapter 3, Addison–Wesley, New York, 1994.
[27] J.S. Brown, Enhanced low energy fusion rate in metal deuterides due to vibrational deuteron dipole–dipole interactions and associated resonant tunneling between neighbouring sites *J. Condensed Matter Nucl. Sci.* **2** (2009) 45–50.
[28] I.P. Chernov, Yu.M. Koroteev, V.M. Silkin and Yu.I. Tyurin, Evolution of the electron structure and excitation spectrum in palladium as a result of hydrogen absorption, *Doklady Phys.* **53**(6) (2008) 318–322, ISSN 1028-3358. © Pleiades Pub. Ltd., 2008. Original Russian Text published in *Doklady Akademii Nauk* **420**(6) (2008) 758–762.
[29] Yu.I. Tyurin and I.P. Chernov, Nonequilibrium escape of atomic hydrogen from metals exposed to radiation, *Dokl. Phys.* **44** (1999) 427–431 [*Dokl. Akad. Nauk* **367** (1999) 328].

J. Condensed Matter Nucl. Sci. 8 (2012) 115–123

Research Article

Electrochemistry and Calorimetry of Ruthenium Co-deposition

Melvin H. Miles*

Dixie State College, St. George, Utah 84770, USA

Abstract

The electrochemical co-deposition of ruthenium (Ru) proved challenging due to the numerous possible oxidation states of this metal. Ruthenium (III) nitrosylnitrate, $Ru(NO)(NO_3)_3$, was investigated in the $NH_4Cl + NH_4OH/H_2O$ and $ND_4Cl + ND_4OD/D_2O$ electrolytes. The ruthenium solution had an intense red color that remained unchanged during extensive electrolysis at constant currents of 6, 10, 20 and 100 mA. However, at a constant current of 400 mA, the solution became completely clear overnight with a black deposit of ruthenium metal covering the copper cathode. The collapsed cyclic voltammetric trace indicated a large electrode capacitance (1–2 F) and a large ruthenium surface area (10^5 cm^2) similar to the previous observations for palladium co-deposition in this ammonia system. Extensive calorimetric studies using a constant current of 200 or 300 mA produced no measureable excess power in H_2O or D_2O for this ruthenium system. The very stable calorimetry allowed the determination of the effect of the electrolyte level on the cell constant at 0.0008 W/K mL for both the Ru/H_2O and the Ru/D_2O systems. The mean cell constants were 0.1318 ± 0.0025 W/K for the Ru/H_2O study and 0.1312 ± 0.0025 W/K for the Ru/D_2O experiment. There was no chemical excess power or shuttle reactions due to the nitrate ions present in these ruthenium solutions. In contrast to the palladium co-deposition studies, there was no detection of chlorine or nitrogen trichloride formation in any ruthenium co-deposition study. Based on out-gassing observations when the current was turned off, there was no absorption of hydrogen or deuterium within the bulk of the deposited ruthenium metal. Preliminary results are also reported for co-deposition studies of rhenium (Re), iridium (Ir), and nickel (Ni). Based on these new experiments with various metals, both palladium and D_2O are essential for excess power in co-deposition studies.
 ISSN 2227-3123

Keywords: Absorption, Capacitance, Cell constants, Oxidation states, Vacancies

1. Introduction

Previous co-deposition calorimetric experiments in the $ND_4Cl + ND_4OD/D_2O$ electrolyte have focused solely on the Pd/D system [1,2]. However, if the anomalous excess power is due to near surface effects or vacancies, then other metals may also be active in producing excess power in co-deposition experiments. The use of other metals will also allow for the testing of the calorimetric system under conditions similar to those for the Pd/D co-deposition system. Ruthenium was selected because this metal was previously investigated as a supercapacitor material [3]. It has been proposed

*E-mail: melmiles1@juno.com

 ISSN 2227-3123

that the large electrochemical capacitance effects observed for ruthenium may involve hydrogen ion absorption into the metal as well as adsorption at the surface [3]. Similar to platinum and palladium, ruthenium is also an excellent catalyst for water electrolysis, fuel cells and other processes. Ruthenium has the electronic configuration $[Kr]4d^75s^1$ and exhibits various oxidation states in its compounds. The most common oxidation state is 3+ as found for $Ru(NO)(NO_3)_3$. This is explained by the loss of two electrons from the 4d level and one electron from the 5s level to give the more stable electronic configuration $[Kr]4d^55s^0$. Other oxidation states for ruthenium are 4+ as illustrated by RuO_2, 8+ as found for the toxic RuO_4, as well as 2+, 5+, 6+, and 7+ oxidation states [4]. The seven oxidation states for ruthenium are tied with osmium as the most for any metal [4]. Another major reason for this ruthenium experiment is that it may serve as a control regarding possible chemical excess heat due to shuttle reactions in the ND_4Cl + ND_4OD + D_2O co-deposition system [5–7]. This study will also provide a comparison between the similarities and differences encountered in palladium and ruthenium co-deposition systems.

2. Experimental

Calorimetric studies used a new isoperibolic design as previously reported [8,9]. Electrochemical experiments such as cyclic voltammetry (CVA) and electrochemical impedance spectroscopy (EIS) were performed using the Princeton Applied Research PARSTAT 2272 with the appropriate software as described elsewhere [6]. The deuterated chemicals used were Cambridge Isotope Laboratories D_2O (99.9 atom % D), ACROS ND_4Cl (98 atom% D), and ACROS ND_4OD (99 atom% D). Alfa-Aesar ruthenium (III) nitrosylnitrate, $Ru(NO)(NO_3)_3$, was used for the electrochemical deposition of ruthenium metal. The actual solution concentrations were 0.02534 M $Ru(NO)(NO_3)_3$, 0.1468 M ND_4Cl, and 0.45 M ND_4OD for the Ru/D_2O study and 0.02158 M $Ru(NO)(NO_3)_3$, 0.1502 M NH_4Cl, and 0.45 M NH_4OH for the Ru/H_2O study.

3. Results

3.1. Electrochemical deposition of ruthenium

The electrochemical deposition of ruthenium from the $Ru(NO)(NO_3)_3$ + NH_4Cl + NH_4OH/H_2O solution proved to be much more difficult than the deposition of palladium from this ammonia system. This was likely due to the multiple of oxidation states for ruthenium. The NH_4Cl + $Ru(NO)(NO_3)_3$ dissolved readily in H_2O to form a dark red solution with pH = 2.53. This acidic ruthenium solution was stable towards displacement reactions for all metals that were tested (Cu, Ni, Co, Al, Ta, Mo, Hf, Ag and Pt). Therefore, metal ion impurities due to chemical reactions should not be a concern in these ruthenium solutions. The addition of 0.15 M NH_4OH did not produce the expected precipitate, thus the NH_4OH concentration was increased to 0.45 M. The solution remained dark red and gave no precipitate with the pH = 9.67. The intense red color of the ruthenium solution remained unchanged during extensive electrolysis at constant currents of 6, 10, 20 and 100 mA. Finally, at a constant current of 400 mA, the ruthenium solution became completely clear overnight with a robust deposit of black ruthenium metal covering the copper cathode. The measured pH of the solution also decreased to pH = 2.02. This is similar to the pH effects observed for palladium co-deposition [6]. The acidic solution produced (pH = 2.02) is due to the cell reaction

$$2Ru^{+++} + 3H_2O \rightarrow 2Ru + 3/2O_2 + 6H^+, \tag{1}$$

where each Ru^{+++} ion deposited is replaced by three hydrogen ions to maintain charge neutrality. Furthermore, the electrolysis gases at high currents drive off the ammonia. There was no detection of chlorine evolution or the related formation of nitrogen trichloride, NCl_3, as previously observed for palladium deposition in this ammonia electrolyte [5,6]. However, this Cl_2/NCl_3 phase may have been passed through quickly overnight at 400 mA. Based on the initial Ru^{+++} concentration in H_2O (0.02158 M), the expected final pH would be 1.19. The higher measured pH = 2.02 could

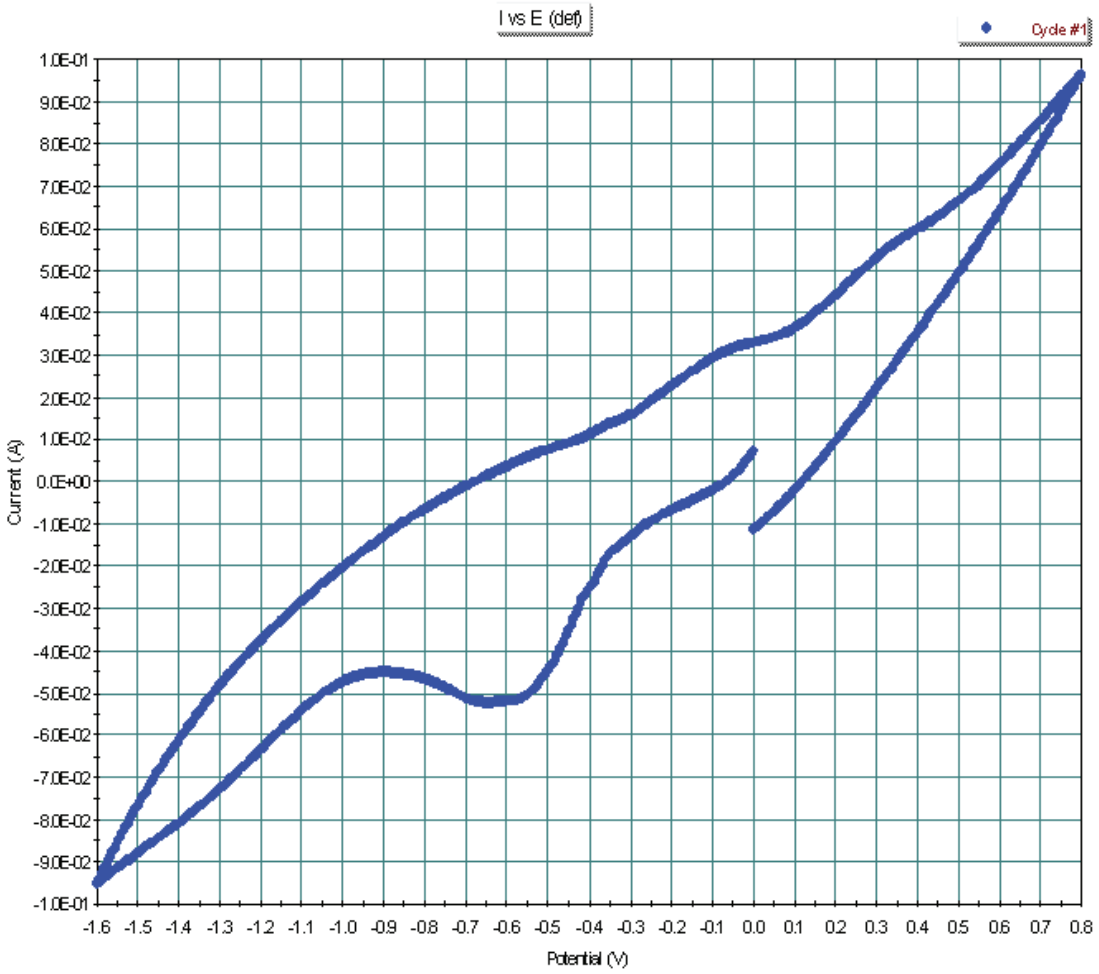

Figure 1. Cyclic voltammetric study prior to the completed ruthenium deposition. The potential sweep rate was 50 mV/s.

be due to some chlorine evolution. Another possibility is the oxidation of small amounts of ruthenium ions to form the volatile and toxic RuO_4 that may exit the cell.

3.2. Electrochemical investigations

The cyclic voltametric study of the cathode before the completed ruthenium deposition is shown in Fig. 1. The solution was still dark red in color, but the copper cathode was completely black due to the partial ruthenium deposition. This study was made following the application of a constant current of 100 mA for 24 h. The reduction peak at −0.63 V may be due to the reduction of Ru^{+++} ions to Ru^{++} or Ru metal. The small oxidation partial peak at −0.05 V could be due to Ru^{++} oxidation back to Ru^{+++}. However, this cyclic voltammogram appears to be partially tilted and collapsed

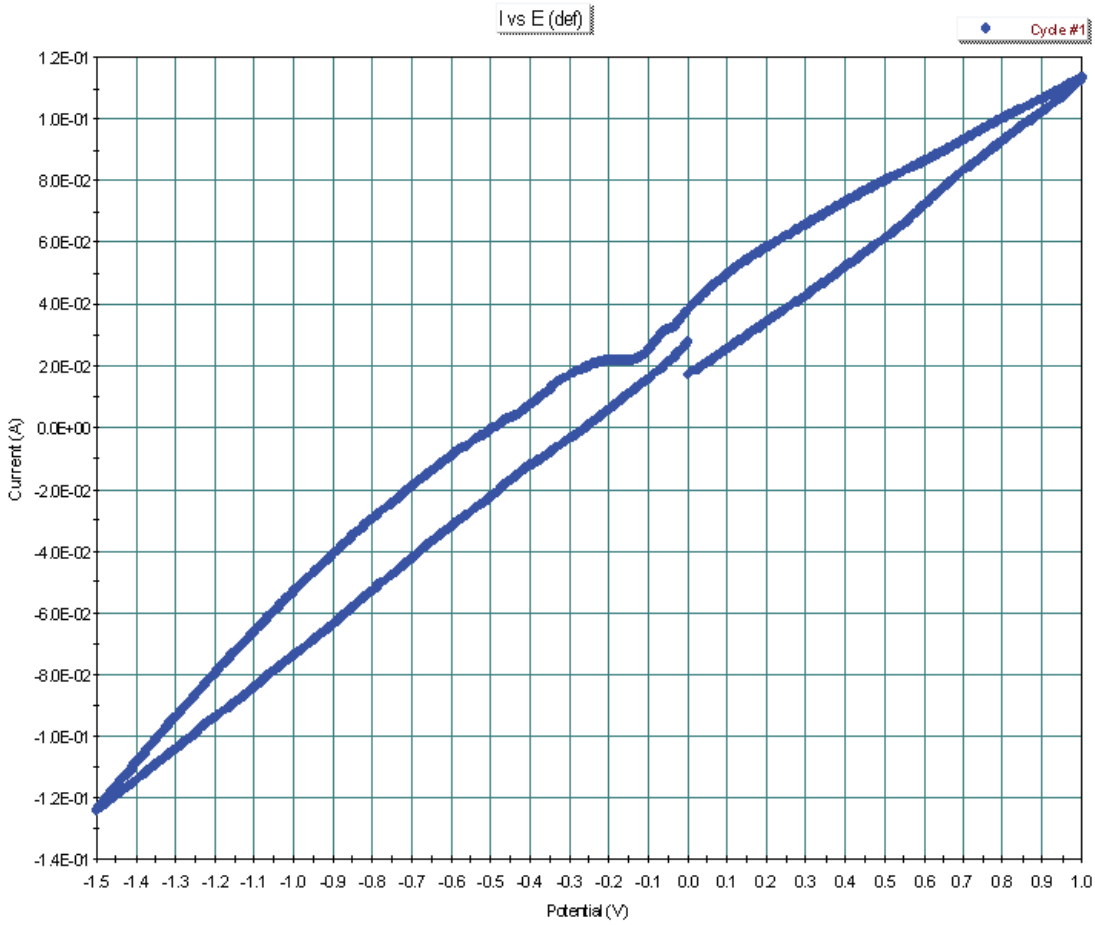

Figure 2. Collapsed and tilted cyclic voltammetric trace following the complete deposition of ruthenium (50 mV/s).

towards Ohm's law behavior due to a large capacitance effect as previously reported for palladium deposition [5]. A reasonable cell resistance of 8.312 Ω can be calculated from the cell currents and voltages at the end points.

Figure 2 presents the cyclic voltammetric study following the complete deposition of ruthenium at a constant current of 400 mA. The cyclic voltammogram is now almost completely tilted and collapsed into a featureless Ohm's law behavior as found for palladium deposition [5,6]. A cell resistance of 10.52 Ω is calculated from the end points for the cell currents and voltages using Ohm's law. This result indicates a capacitance of about 1–2 F for the ruthenium cathode and a surface area of about 10^5 cm^2 (Refs. [3,5]).

Figure 3 presents the Nyquist plot for an EIS study after further electrolysis at 50 mA over the weekend. A reasonable semicircle is observed followed by the beginning of a larger semicircle at lower frequencies. The EIS results suggest good electrode kinetics due to the larger surface area and also provides an accurate value of 14.25 Ω for the cell resistance. From the measured charge transfer resistance (R_{ct}) of 3.30 Ω, an exchange current of 4×10^{-3} A is calculated for the electrode reaction at open circuit.

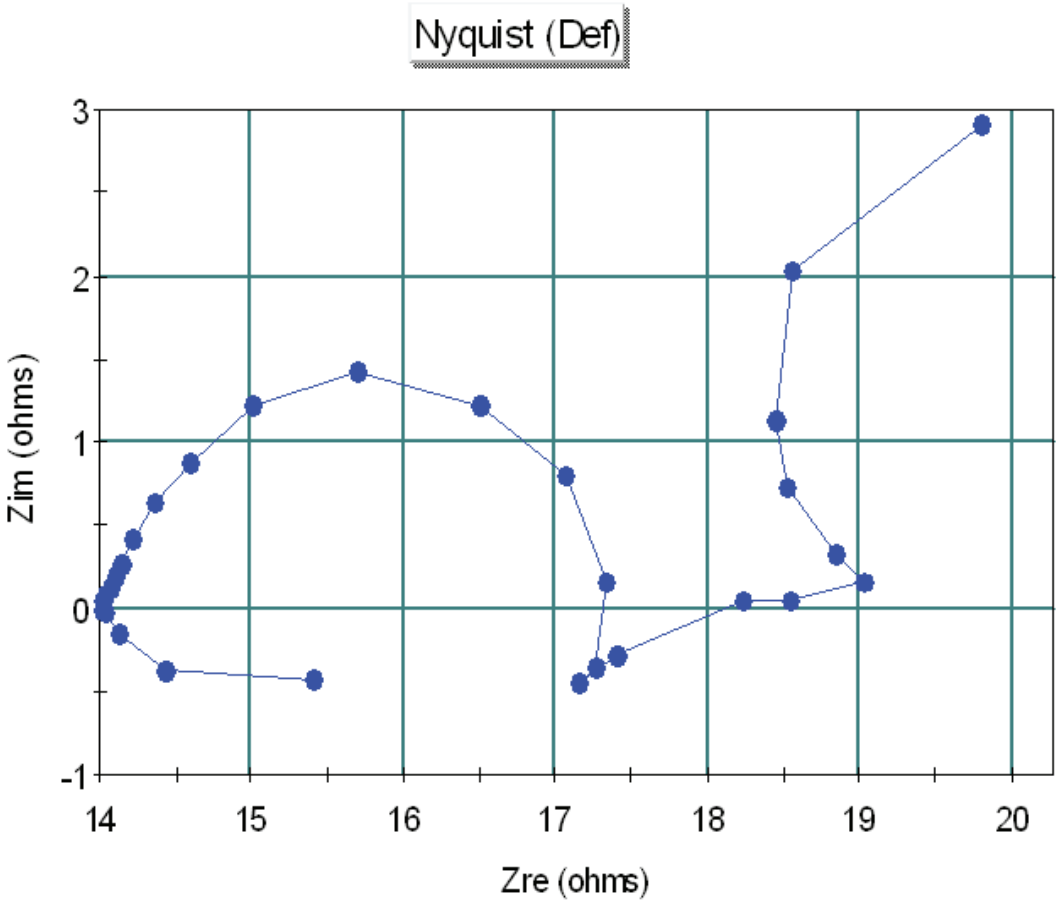

Figure 3. Nyquist plot for an EIS study after further electrolysis. The frequency range was from 100 kHz to 10 mHz.

3.3. Calorimetry

The simplest starting point for calorimetric measurements is (Refs. 8–10)

$$P_x = (k_C - k'_C)\Delta T, \tag{2}$$

where P_x is the excess power, k_C is the true conductive heat transfer coefficient, k'_C is the lower bound conductive heat transfer coefficient obtained by assuming $P_x = 0$. Obviously k_C and k'_C would be identical if there were actually no excess power. The advantage of this simple equation is that all other calorimetric power terms cancel in this derivation [8–10]. For the calorimeter used in this study, the true conductive heat transfer coefficient has been established as 0.1340 W/K when the electrochemical calorimetric cell is filled with 50.0 mL of electrolyte. This cell constant will decrease as the electrolyte level decreases during electrolysis.

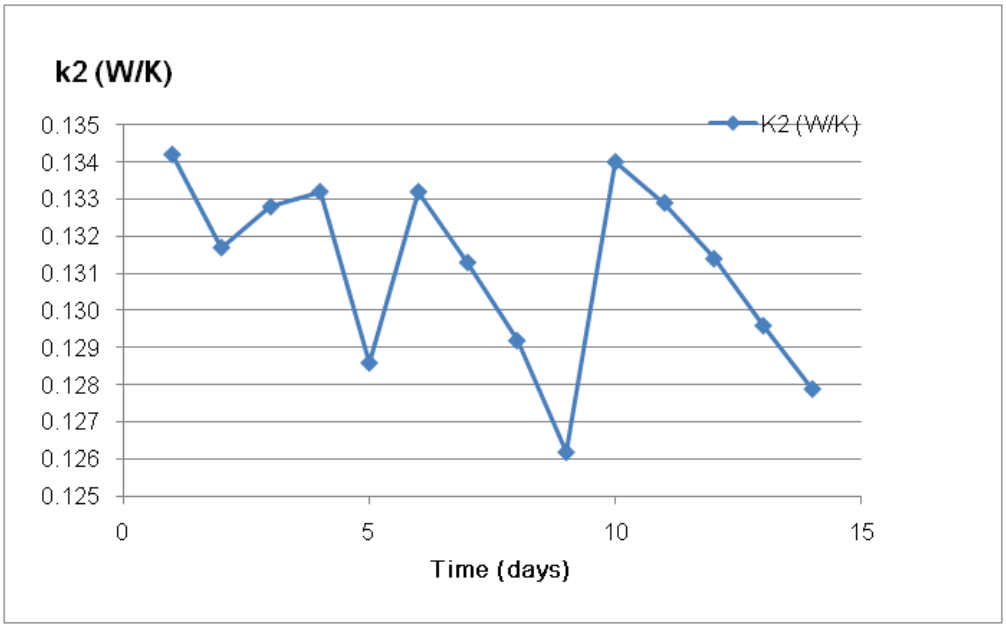

Figure 4. Calorimetric lower-bound conductive heat transfer coefficient (k_2) versus time for the Ru/H_2O experiment in the NH_4Cl + NH_4OH/H_2O electrolyte.

Figure 4 presents the lower-bound conductive heat transfer coefficient (k_2) measured using Thermistor 2 for the Ru/H_2O experiment in the ammonia (NH_4Cl + NH_4OH/H_2O) electrolyte.

This calorimetric study at a constant current of 300 mA shows only the expected changes of the cell constant due to changes in the electrolyte level. The peaks show where make-up H_2O was added to the cell. These results are for Thermistor 2 used in the calorimeter. A second thermistor (Thermistor 4) positioned on the opposite side of the electrochemical cell provided results (k_4) similar to those of Fig. 4.

Figure 5 shows the lower-bound heat transfer coefficient (k_2) for the Ru/D_2O experiment in the ND_4Cl + ND_4OD/D_2O electrolyte. This cell started with an over-filled electrolyte level of about 55 mL, thus the cell constant (k_2) is higher at the beginning. Also, lower currents of 200 and 250 mA were used during the first few days. Nevertheless, the results in Fig. 5 are very similar to those shown in Fig. 4. Both the Ru/H_2O and the Ru/D_2O studies were run longer than normal between cell re-filling in order to measure the effect of the electrolyte level in these stable calorimetric experiments. Much smaller changes in k_2 would occur with the normal cell filling every 1 or 2 days.

As shown in Figs. 4 and 5, there are no significant differences between the Ru/H_2O and the Ru/D_2O experiments because neither study produced excess power. In fact, the mean calorimetric cell constants are almost identical. For Ru/H_2O, the mean cell constant is $\langle k_2 \rangle = 0.1318 \pm 0.0030$ W/K while $\langle k_2 \rangle = 0.1312 \pm 0.0025$ W/K for Ru/D_2O. These mean cell constants are less than the true value of 0.1340 W/K because the mean electrolyte level is less than the initial filled volume of 50.0 mL. The error ranges given for $\langle k_2 \rangle$ reflect the larger than normal changes in the electrolyte volume rather than actual calorimetric errors. The calorimetric stability for these ruthenium studies allowed the measurements of the effect of the electrolyte level on the cell constant, $\Delta k_2/\Delta V$. For both Ru/H_2O and Ru/D_2O, the results were measured as $\Delta k_2/\Delta V = 0.0008 \pm 0.0001$ W/K mL.

3.4. Consumption of H_2O and D_2O

The H_2O or D_2O consumption has been measured in every co-deposition study using the ammonia system. These measured amounts are then compared with the theoretical calculations based on Faraday's law using −9.03 mL/F for H_2O electrolysis and −9.07 mL/F for D_2O electrolysis where F = 96,485 C/eq (C = A s). Previous results are presented elsewhere [6]. In these experiments, the Ru/H_2O study gave a measured H_2O consumption of 45.5 mL versus the theoretical value of 40.7 mL. For the Ru/D_2O study, the measured consumption of D_2O was 43.0 mL versus the theoretical value of 41.8 mL. The ratio of measured/theoretical is 1.12 for Ru/H_2O and 1.03 for Ru/D_2O. This is consistent, within error limits, of previous studies [6]. Including these ruthenium results with six previous palladium studies [6] yields a mean measured/theoretical ratio of 1.083 ± 0.099. None of these consumption measurements suggest any significant recombination of the electrolysis gases or any significant shuttle reactions [6]. This measured/theoretical ratio is expected to be somewhat larger than unity due to H_2O or D_2O evaporation where the vapor exits the cell with the electrolysis gases [10]. The exact value of this ratio is largely determined by the temperature of the vapor at the glass exit tube.

4. Discussion

4.1. Ruthenium red

The difficulty of the electrochemical deposition of ruthenium and the deep red solution color is likely due to the formation of the inorganic dye "Ruthenium Red" [4]. This substance, $[(NH_3)_5$–Ru-O-Ru$(NH_3)_4$-Ru$(NH_3)_5]^{6+}$ is produced by the treatment of "$RuCl_3$" with aqueous ammonia in air [4]. These conditions were certainly present in these experiments using the ammonia and ammonium chloride electrolyte and the production of oxygen at the anode. Two Ru atoms are in the 3+ oxidation and one is in the 4+ oxidation state in this substance. High over-voltages produced by high currents are likely needed to break up this stable substance and reduced the "Ruthenium Red" ruthenium ions to the metal. This

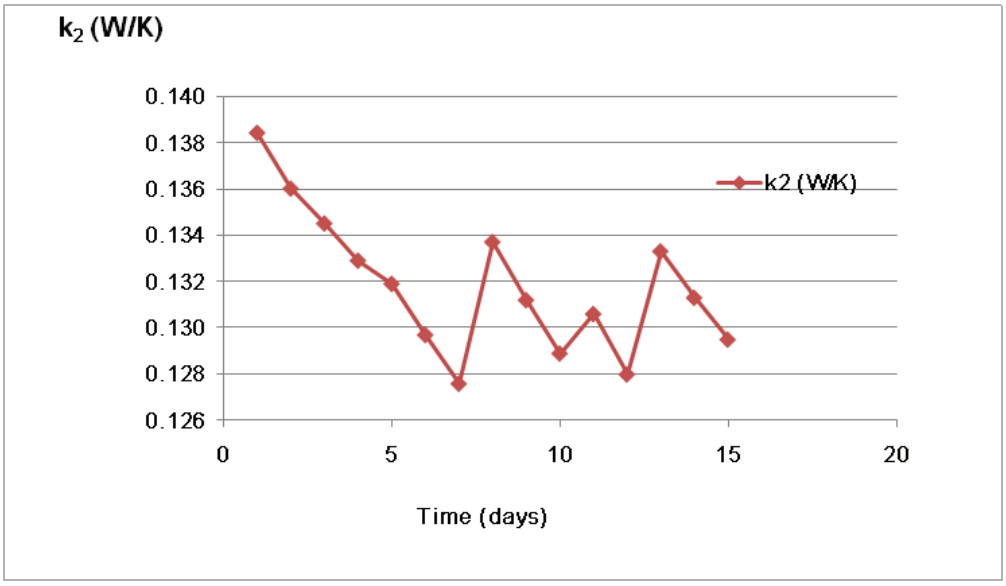

Figure 5. Calorimetric lower-bound heat transfer coefficient (k_2) versus time for the Ru/D_2O experiment in the $ND_4Cl + ND_4OD/D_2O$ electrolyte.

is very different from the palladium co-deposition system where the reduction of palladium ions occurs readily at low currents.

4.2. Nitrate ions

The 0.025 M $Ru(NO)(NO_3)_3$ dissolves to form 0.075 M NO_3^- in H_2O or D_2O solutions. It has been proposed that nitrate ions may form from the NH_4Cl + NH_4OH solutions and undergo shuttle reactions that give an excess power effect [5–7]. The lack of any excess power effect in these studies despite the presence of nitrate ions provides further evidence against proposed shuttle reactions in this ammonia based co-deposition systems [5,6].

4.3. Electrolyte level effect

The ruthenium experiments that gave the electrolyte level effect of $\Delta k_2/\Delta V = 0.0008$ W/K mL involved the usual 50.0 mL of the heat conducting fluid (Mobile-1 oil) surrounding the glass electrochemical cell within the calorimeter [8]. This heat conducting fluid was, therefore, always above the electrolyte level in the cell. In the next experiment with rhenium, only 35.0 mL of the heat conducting fluid was added. This simple change reduced the electrolyte level effect by about a factor of four to yield 0.0002 W/K ml. Maintaining the electrolyte level above the level of the heat conducting fluid maintains a constant surface area for the main heat transfer pathway from the electrolyte across the heat conducting fluid and cell insulation to the water bath. This principle is similar to the Fleischmann–Pons Dewar cell that is silvered at the top in the region of the electrolyte level to maintain a constant surface area for radiative heat transfer [10]. When properly filled, the electrolyte level is at the mid-point of the silvered region for the Dewar cell [10]. The silvered region does not support radiative heat transfer in the Dewar cell. Similarly, the regions filled with air or electrolysis gases in this copper calorimeter are not nearly as effective as the liquid phases for heat transfer by conduction. Providing a constant surface area for heat transport is an important feature for accurate isoperibolic calorimeters.

4.4. Role of vacancies

Metal vacancies created in co-deposition experiments may be important for the excess power effect [11]. The creation of vacancies during the co-deposition of metals mainly requires the absorption of hydrogen or deuterium into the metal lattice to give a high H/M or D/M ratio where M represents a metal [11]. Based on this study, ruthenium produces very little absorption of H or D into the metal. Unlike palladium, the outgassing of hydrogen from ruthenium stopped abruptly when the current was switched off. This observation agrees with ruthenium studies at high hydrogen pressures (90 kbar) that gave only very small ratios of H/Ru = 0.03 [12]. Therefore, the low level of acceptability of hydrogen into the ruthenium lattice and the resulting low level of vacancies may explain why there was no measurable excess power for the Ru/D co-deposition system.

4.5. Preliminary results for the co-deposition of other metals

Initial studies for the co-deposition of rhenium (Re), iridium (Ir), and nickel (Ni) have been completed using the same ammonia electrolyte as used for palladium and ruthenium. No measurable excess power was detected in the calorimetric studies. The compounds used were $ReCl_3$, $IrCl_3$, NiO, and $NiCl_2{\cdot}6\ H_2O$. Low cell currents (6–10 mA) were used for Re and Ir deposition as well as for the study using NiO. However, a much larger deposition current of 200 mA was used for the $NiCl_2{\cdot}6\ H_2O$ experiment. None of these metals showed any significant hydrogen absorption based on out-gassing observations. In fact, iridium is one of the most resistive metals to hydrogen absorption with H/Ir = 0.005 even at 90 kbar (90,000 atm) hydrogen pressure at 250°C [12].

It should be noted that the complete deposition of the metal was achieved in all studies except for the iridium solution where a black precipitate remained. However, about half of the iridium was deposited onto the cathode in the usual black form. The statistical analysis of all 19 co-deposition experiments involving Pd, Ru, Re, Ni and Ir in H_2O and D_2O yields a probability of greater than 99.9999% that the anomalous excess power effect in these co-deposition studies requires the presence of both palladium metal and D_2O. The probability that these results showing excess power only for the Pd/D co-deposition systems could be due to random errors calculates to be less than one in a million.

5. Summary

The electrochemistry and chemistry of the ruthenium co-deposition system varied markedly from the palladium system. However, the black metallic deposit, the high surface capacitance, the high electrode area produced, the H_2O and D_2O consumption, and the large changes in the solution pH were similar. However, no excess power was observed for the Ru/D system. This is likely due to the low level of acceptability of hydrogen or deuterium into the ruthenium metal lattice. The very stable calorimetry for the ruthenium co-deposition system permitted accurate measurements of the electrolyte level effect on the calorimetry.

Acknowledgements

The author thanks the New Energy Foundation, Concord, NH for a donation to purchase the PAR Model 362 Scanning Potentiostat used in the calorimetric studies. Financial support of this work was from an anonymous fund at the Denver Foundation. Dixie State College of Utah and the Dixie Foundation, especially Kalynn Larson, assisted in the administration of this fund.

References

[1] S. Szpak, P.A. Mosier-Boss, and M.H. Miles, Calorimetry of the Pd + D Co-Deposition, *Fusion Technol.* **36** (1999) 234.
[2] S. Szpak, P.A. Mosier-Boss, M.H. Miles, and M. Fleischmann, Thermal behavior of polarized Pd/D electrodes prepared by co-deposition, *Thermochimica Acta* **410** (2004) 101.
[3] M.H. Miles, T.J. Groshens, and C.E. Johnson, Examination of linear potential sweep methods in determining the capacitance of hydrous ruthenium oxide materials, in *Batteries and Supercapacitors*, edited by G.A. Nazri, E. Tekeuchi, R. Koetz and B. Scrosati, PV 2001, The Electrochemical Society Inc., Pennington, NJ, pp. 602–609 (2001).
[4] N.N. Greenwood and A. Earnshaw, *Chemistry of the Elements*, Pergamon Press, Oxford, U.K., First Edition, pp. 1242–1274 (1984).
[5] M.H. Miles, Investigations of co-deposition systems, *Proceedings of ICCF-15*, ENEA, Rome, Italy, 2009, pp. 33–37.
[6] M.H. Miles, Investigations of possible shuttle reactions in co-deposition systems, *Proceedings of ICCF-16*, Chennai, India, 2011 (submitted).
[7] D. Knies, Personal Communication (2009).
[8] M.H. Miles and M. Fleischmann, New approaches to isoperibolic calorimetry, *ICCF-15 Proceedings*, ENEA Rome, Italy, 2009, pp. 22–26.
[9] M.H. Miles and M. Fleischmann, Measurements of excess power effect in Pd/D_2O systems using a new isoperibolic calorimeter, *J. Condensed Matter Nuclear Sci.* **4** (2011) 45–55.
[10] M.H. Miles, M. Fleischmann, and M.A. Imam, *Calorimetric Analysis of a Heavy Water Electrolysis Experiment Using a Pd-B Cathode*", Report Number NRL/MR/6320-01-8526, Naval Research Laboratory, Washington, DC, March 26 (2001).
[11] P. Hagelstein, *E-mail Communications*, June (2011).
[12] V.E. Antonov, I.T. Belash, V.Yu. Malyshev, and E.G. Ponyatovsky, The Solubility of Hydrogen in the Platinum Metals Under High Pressure, *Int. J. Hydrogen Energy* **11**(3) (1986) 193.